6-9-2008

Electrical Actuation of Dielectric Droplets

Niru Kumari
Birck Nanotechnology Center and School of Mechanical Engineering, Purdue University, nkumari@purdue.edu

Vaibhav Bahadur
Purdue University - Main Campus, vbahadur@purdue.edu

S V. Garimella
Purdue University, sureshg@purdue.edu

Follow this and additional works at: http://docs.lib.purdue.edu/coolingpubs

Electrical actuation of dielectric droplets

N Kumari, V Bahadur and S V Garimella[*]

School of Mechanical Engineering and Birck Nanotechnology Center
Purdue University
West Lafayette, IN 47907-2088
USA

Abstract

Electrical actuation of liquid droplets at the microscale offers promising applications in the fields of microfluidics and lab-on-a-chip devices. Much prior research has targeted the electrical actuation of electrically conducting liquid droplets; however, actuation of dielectric droplets has remained relatively unexplored, despite the advantages associated with the use of a dielectric droplet. This paper presents modeling and experimental results on the electrical actuation of dielectric droplets between two flat plates. A first-order analytical model, based on the energy-minimization principle, is developed to estimate the electrical actuation force on a dielectric droplet as it moves between two flat plates. Two versions of this analytical model are benchmarked for their suitability and accuracy against a detailed numerical model. The actuation force prediction is then combined with available semi-analytical expressions for predicting the forces opposing droplet motion to develop a model that predicts transient droplet motion under electrical actuation. Electrical actuation of dielectric droplets is experimentally demonstrated by moving transformer oil droplets between two flat plates under the influence of an actuation voltage. Droplet velocities and their dependence on the plate spacing and the applied voltage are experimentally measured and showed reasonable agreement with predictions from the models developed.

Keywords: electrical actuation, dielectric droplet, energy minimization, microfluidics, electrowetting

---

[*] Corresponding author: E-mail: sureshg@purdue.edu

1. Introduction

Electrical actuation and control of fluid motion at the microscale has significant applications in the areas of microfluidics and lab-on-a-chip devices. Electrical actuation of electrically conducting droplets has received significant research attention over the past decade. Electrowetting (EW) [1], for example, has been extensively studied [2- 7] as a tool to actuate and control electrically conducting droplets.

Many microelectronics applications which involve direct contact of the liquid with an electronic component would require the use of electrically insulating liquids. Insulating liquids are also typically much less corrosive than electrically conducting alternatives. A scaling analysis reveals that the actuation voltage required to move an electrically insulating droplet is significantly higher than that for an electrically conducting droplet. Despite the high voltages, however, the use of insulating liquids is the only viable option for applications in which electrically conducting liquids may not be used. Very little published work is available on the electrical actuation of dielectric fluid elements. Pellat [8] performed a classic experiment in 1895 which consisted of drawing up a finger of transformer oil between two parallel plates through the application of an electrical voltage. Jones *et al.* [9] demonstrated a rise in the height of a transformer oil finger (between two parallel plates with a separation of 1 *mm*) upon the application of an AC voltage. No studies in the literature have considered electrical actuation of dielectric fluid *droplets*.

The study of electrical actuation of dielectric liquid droplets can build upon the extensive research studies available in the field of electrowetting-induced droplet movement. Phenomena which influence EW systems such as contact-line friction are also important in dielectric droplet actuation. The actuation forces on an electrically conducting droplet and a dielectric droplet have a common electromechanical origin [9] and can be analyzed using the principle of energy minimization. Additionally, the flow fields in an electrically conducting droplet and a dielectric droplet are expected to be similar. Consequently, much of the knowledge of EW-induced conducting droplet motion can be directly applied to the study of dielectric droplet actuation. Electrowetting has been used to demonstrate droplet actuation [4, 5, 10- 16] and other microfluidic operations such as the formation, mixing and splitting of droplets [17]. There has also been good progress in understanding the physics governing phenomena which influence EW systems, such as contact angle saturation [18], role of the electrical double layer [19] and dynamics of the three-phase line [20].

The primary objective of this paper is to obtain the electrical actuation force on a dielectric droplet as it moves between two flat plates using an energy-minimization framework [2, 6, 7, 21]. In the case of the dielectric droplet considered, the electric field lines penetrate into the droplet which significantly increases the complexity of the analysis relative to conducting droplets, since energy storage occurs inside the droplet as well as the dielectric layer. An analytical model is developed to obtain first-order estimates of the actuation force, and compared to results from a rigorous numerical analysis. The analytical model enables the influence of actuation voltage, droplet geometry and dielectric parameters on the actuation force to be clearly understood. The numerical actuation force model is then combined with semi-empirical expressions [2] for the forces opposing droplet motion to arrive at predictions of the transient motion of a dielectric droplet. A parallel experimental effort is carried out to demonstrate electrical actuation of a dielectric droplet; the experimental results are also used to validate the models developed in the present work.

2. Energy-based models for dielectric droplet motion

2.1 *Representative droplet actuation device*

A representative device used for electrical actuation of dielectric droplets is shown in Figure 1 and is similar to the configuration used for EW-induced actuation of electrically conducting liquids [2]. It consists of two flat plates separated by a known spacing. An array of electrodes on the bottom plate is used to actuate the droplet. The top plate has a continuous electrode which serves as the ground electrode and ensures complete droplet transition to the actuated electrode [2]. The electrodes on the bottom plate are covered with a dielectric layer which prevents chemical reactions between the ions in the droplet and the metal electrodes. The top plate does not have a dielectric layer which maximizes the electrical actuation force on the droplet [2]. A hydrophobic layer of Teflon is coated on both plates to ensure high initial contact angles.
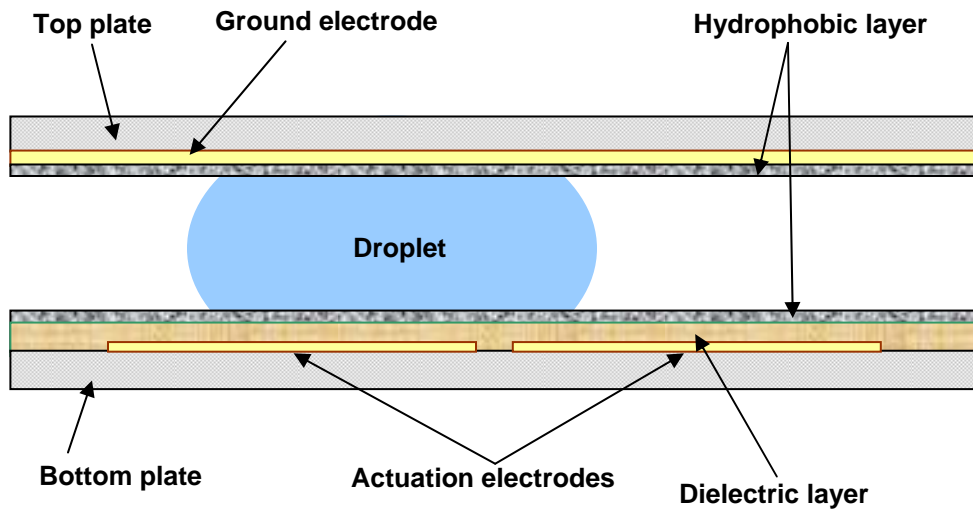

Figure 1. Representative device for electrical actuation of dielectric droplets.

### 2.2 *Analytical model for dielectric droplet actuation force*

The energy-minimization framework developed by Bahadur and Garimella [2] for electrically conducting droplets is utilized in the present work; however, the treatment of a dielectric droplet is significantly different because of the capacitive energy stored in the droplet itself. In the case of a dielectric droplet, the capacitive energy storage in the droplet is significant and needs to be accounted for in the energy-minimization framework. The droplet (of radius r) is sandwiched between the two plates with a separation of H as shown in Figure 2. The top plate and the left electrode on the bottom plate are grounded and the right electrode serves as the actuation electrode. The dielectric thickness covering the bottom electrodes is d_1. The coordinate system to track the leading edge of the droplet is located at the center of the intersection line of the two electrodes on the bottom plate as shown in Figure 2. The droplet is assumed to maintain its circular shape (in plan view) during the transition, and any deformation induced during its movement by contact-line friction is neglected. However, the modeling framework developed in the present work can be used to estimate the actuation force for a droplet of any shape.
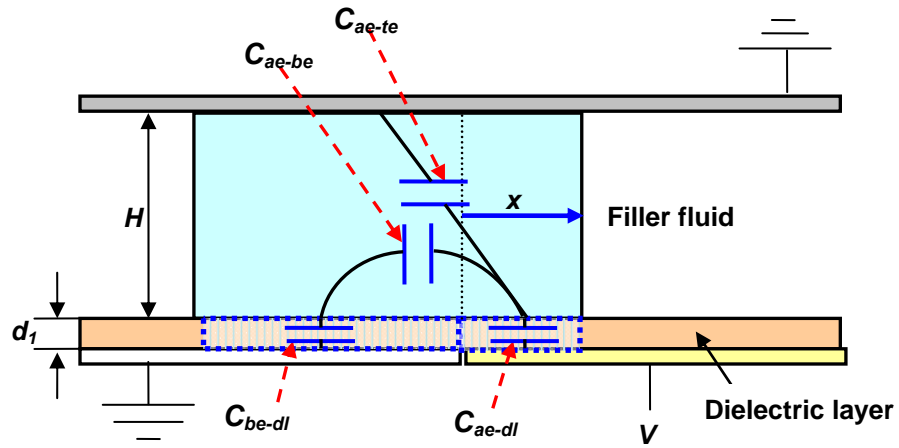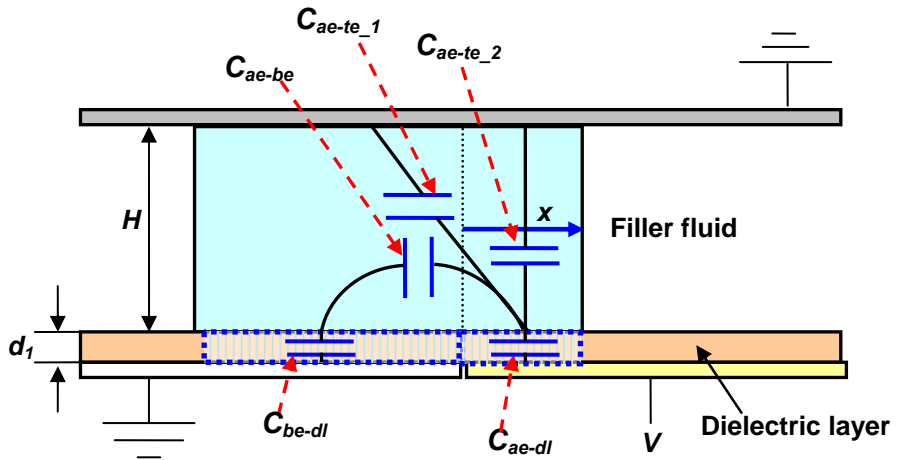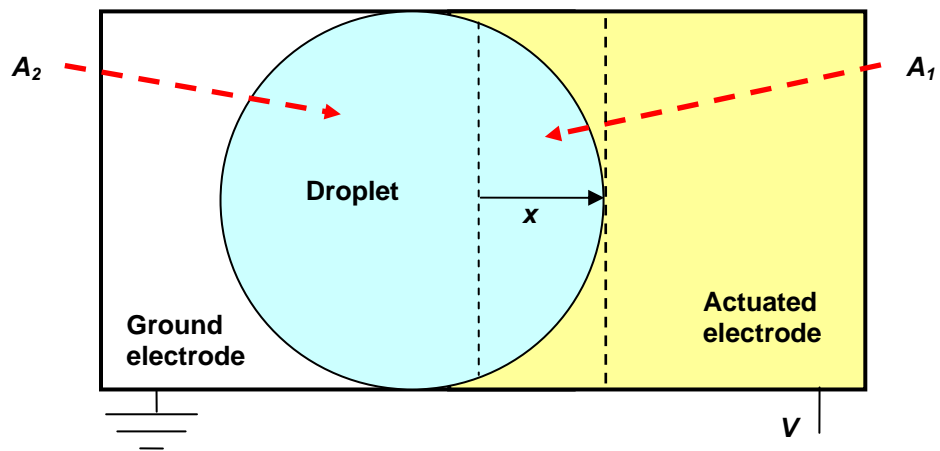
Figure 2. Schematic illustration of a droplet undergoing transition: (a) side view showing analytical approach 1, (b) side view showing analytical approach 2, and (c) top view.

The actuation force is calculated following the approach of Carnero and Carretero [22] to predict the electrical actuation of a rectangular dielectric slab sliding between two plates. The actuation force model is based on a knowledge of the change in capacitive energy of the system as the droplet moves to the actuated electrode. This energy storage occurs within the various capacitances associated with the droplet and dielectric layers shown in Figure 2. The areas covered by the droplet on different electrodes (A_1 on the actuated electrode, A_2 on the grounded bottom electrode, and A_3 on the top plate) required for calculating these capacitances can be determined from the droplet geometry shown in Figure 2(c).

Two versions of the actuation force model follow from the use of two alternative approaches to treat the droplet capacitance as illustrated in Figure 2. Figure 2(a) shows two dielectric layer capacitance elements and two droplet capacitance elements, while Figure 2(b) shows two dielectric layer capacitance elements and three droplet capacitance elements. The capacitance C_{ae-te} of approach 1 is further subdivided in approach 2. The voltage drops across the capacitive layers can be obtained from a capacitive network analysis of the system. All the capacitances are represented as parallel-plate capacitors (Figure 2a and 2b) to form the capacitive networks shown in Figure 3a and 3b. The electric field lines in all the parallel-plate capacitors are assumed to be perfectly straight and fringing effects at the sides are not accounted for in the present model. It is also important to note that the electrostatic energy stored in the filler fluid medium (air) around the droplet is not estimated in the present analytical model. The energy storage in the surrounding air can be neglected when the dielectric constant of the droplet is significantly greater than the dielectric constant of air.

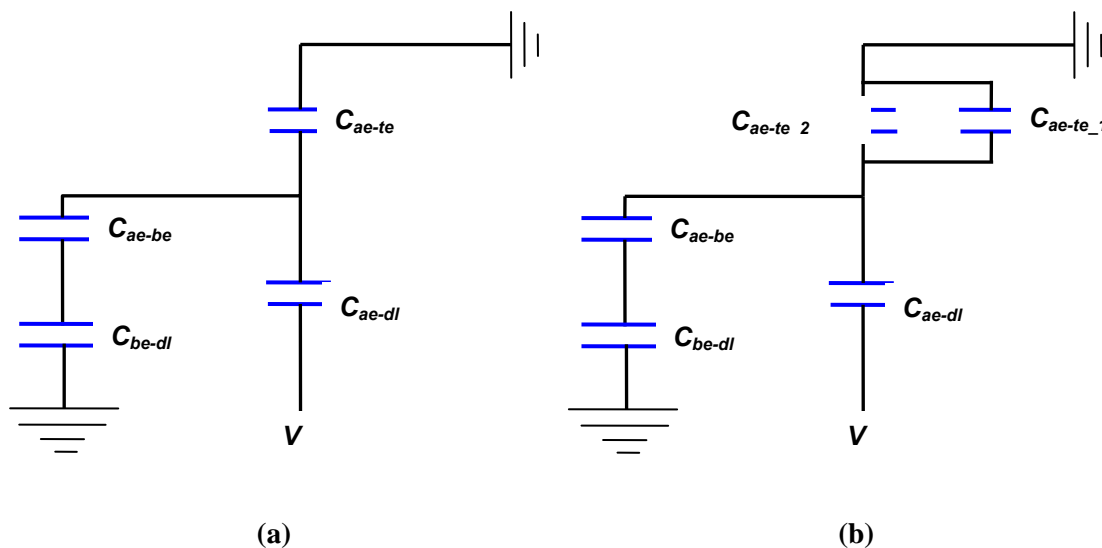(a)   (b)

**Figure 3. Capacitive network for the estimation of voltages across the capacitive elements:
(a) analytical approach 1, and (b) analytical approach 2.**

The capacitances associated with the first analytical approach above (Figure 3a) are as follows:

$$C_{ae-dl}(x) = \frac{k_1 A_1(x)\varepsilon_0}{d_1} \tag{1}$$

$$C_{ae-te}(x) = \frac{k_d \left(A_1(x) + A_3(x) \right) \varepsilon_0}{2d_{ae-te}} \tag{2}$$

$$C_{ae-be}(x) = \frac{k_d \left(A_1(x) + A_2(x) \right) \varepsilon_0}{2d_{ae-be}} \tag{3}$$

$$C_{be-dl}(x) = \frac{k_1 A_2(x) \varepsilon_0}{d_1} \tag{4}$$

where,

$$d_{ae-te} = \sqrt{\left(x_{cent\_A_1} - x_{cent\_A_3} \right)^2 + H^2} \tag{5}$$

$$d_{ae-be} = \pi \frac{\left(x_{cent\_A_1} - x_{cent\_A_2} \right)}{2} \tag{6}$$

$$A_1(x) = r^2 \cos^{-1}\left(1 - \frac{x}{r} \right) - (r-x)\sqrt{r^2 - (x-r)^2} \tag{7}$$

$$A_2(x) = \pi r^2 - A_1(x) \tag{8}$$

$$A_3(x) = \pi r^2 \tag{9}$$

In the above equations, k_1 is the dielectric constant of the dielectric layer, d_1 is the dielectric layer thickness, k_d is the dielectric constant of the droplet and H is the spacing between the two plates as shown in Figure 2a. x_{cent_A1}, x_{cent_A2} and x_{cent_A3} are the x-coordinates of the centroids of areas A_1, A_2 and A_3, respectively. The equivalent capacitance $C_{eqv}(x)$ can now be expressed as:

$$\left(C_{eqv}(x) \right)^{-1} = \left(C_{ae-dl} \right)^{-1} + \left(\frac{C_{ae-be} C_{be-dl}}{C_{ae-be} + C_{be-dl}} + C_{ae-te} \right)^{-1} \tag{10}$$

The total electrostatic energy $E(x)$ of the system can be estimated as:

$$E(x) = \frac{1}{2} C_{eqv}(x) V^2 \tag{11}$$

The actuation force acting on the drop during the transition can be estimated as the positive derivative of this energy function as shown by Carnero and Carretero [22]:

$$F_{act}(x) = \left(\frac{dE(x)}{dx} \right)_V \tag{12}$$

In the second analytical approach, the capacitance C_{ae-te} of the first approach is further subdivided into two capacitive elements as shown in Figure 3b. The first component $C_{ae-te-1}$ accounts for energy storage in the part of the droplet between the actuated electrode and its corresponding area on the top plate; the electric field lines in this capacitance are assumed to be straight and perpendicular to the plates. The second component $C_{ae-te-2}$ represents the capacitance between the remaining part of the top plate and the actuated electrode, with the area of the capacitance being the average area of the plates and the plate distance estimated as the centroidal distance between the plates. The two new capacitances introduced in the second approach are given by:

$$C_{ae-te\_1} = \frac{k_d A_1 \varepsilon_0}{H} \tag{13}$$

$$C_{ae-te\_2} = \frac{k_d \left(A_1 + (A_3 - A_1) \right) \varepsilon_0}{2d_{ae-te\_2}} \tag{14}$$

where

$$d_{ae-te\_2} = \sqrt{\left(x_{cent\_A_1} - x_{cent\_A_2}\right)^2 + H^2} \tag{15}$$

The two capacitances described above are in parallel and hence the equivalent capacitance C_{ae-te} can be estimated as:

$$C_{ae-te} = C_{ae-te\_1} + C_{ae-te\_2} \tag{16}$$

The value of C_{ae-te} is used in Eq. (10) and $E(x)$ and $F_{act}(x)$ can be calculated using Eq. (11)-(12).

2.3 Numerical model for droplet actuation force
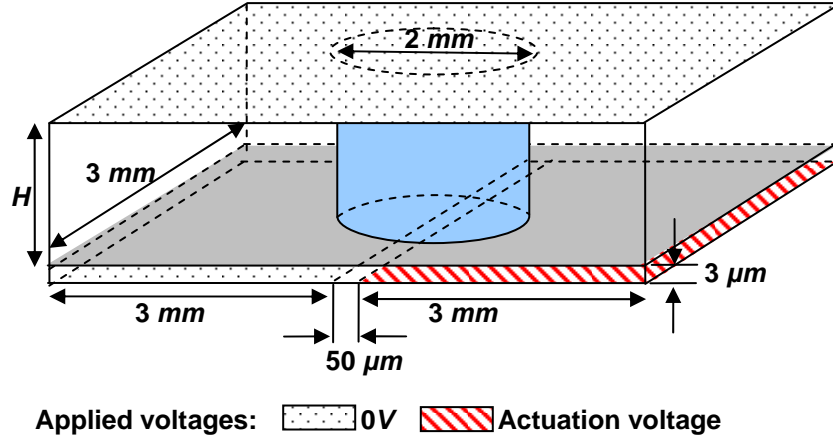

Figure 4. Schematic diagram of the numerical simulation domain.

The analytical modeling above is intended to provide first-order predictions of the actuation force on a dielectric droplet. In order to judge the suitability and accuracy of the analysis, a detailed numerical simulation was carried out. The finite element software package ANSYS [23] was used to simulate the electric field and electrostatic energy distribution in the droplet and the dielectric layer. Figure 4 shows a schematic diagram of the simulation domain which consists of a 2 *mm* diameter droplet between two flat plates with a 3 *μm* dielectric layer on the bottom plate. Electrical actuation voltages were applied through two actuation electrodes at the bottom of the dielectric layer (shown in the form of boundary conditions in Figure 4). A zero voltage boundary condition was specified on the left electrode on the bottom plate and the top plate electrode (Figure 4), while the actuation voltage was applied on the right electrode on the bottom plate. The two actuation electrodes on the bottom plate were 3 *mm* x 3 *mm* in size and were larger than the droplet to facilitate meshing of the domain. The two actuation electrodes were separated by 50 *μm* to emulate a practical system. The total capacitive energy of the system $E(x)$ was calculated at multiple discrete points along the transition path of the droplet from the ground electrode to the actuated electrode. A polynomial curve was then fit to these data points to obtain an expression the energy distribution function $E(x)$. The electrical actuation force $F_{act}(x)$ was then estimated using Eq. (12). It may be noted that the capacitive energy estimation in this numerical framework also includes the energy stored in the filler fluid medium which is air in the present application. The analytical model does not account for the energy storage in the filler fluid medium; however, the contribution of the filler fluid is extremely small because of the very low dielectric constant of the air, and this difference between the numerical and analytical models is not significant. Table 1 shows the geometric parameters and material properties used in the analytical and numerical models discussed.

7

Table 1. Parameters used for actuation force estimation.

Parameter	Value
Droplet radius (r) = half the electrode width	1 mm
Dielectric constant of lower plate dielectric (k_1)	3
Dielectric constant of droplet (k_d)	2.1
Dielectric constant of Parylene C	3
Thickness of lower plate dielectric :(d_1)	3 μm
Plate spacing (H)	100-500 μm
Actuation voltage (V)	1000-1500 V

2.4 Opposing forces and droplet motion

The dominant forces [2] opposing droplet motion are the shear forces due to the top and bottom plates, the viscous drag exerted by the surrounding air, and the contact-line friction. Significant challenges exist in estimating each of these components as described in Reference 2. However, the present work is not aimed at resolving these challenges, and semi-empirical expressions are used to estimate the opposing forces as described in Reference 2.

The differential equation governing droplet motion is then given as:

$$m\frac{d^2x}{dt^2} = F_{act} - \left(\frac{6\mu_l v}{H}\right)(2\pi r^2) - \left(\frac{1}{2}C\rho_f v^2\right)(2rH) - (\zeta v)(4\pi r) \tag{17}$$

where m is the droplet mass. The opposing forces on the right hand side of Eq. (17) are as follows. The first is the viscous force on the droplet due to the top and bottom plates (v is the droplet velocity and μ_l is the droplet viscosity). The second is the viscous stress due to the filler fluid, which is estimated by considering the droplet as a rigid body moving through the filler fluid (C is the drag coefficient for a cylinder in cross flow and ρ_f is the filler fluid density). The third opposing force is the contact-line friction force, which is assumed to be proportional to the droplet velocity as suggested by Ren et al. [24]. ζ is a proportionality coefficient which depends on the droplet-surface combination. The physical properties of transformer oil used in the droplet motion model are listed in Table 2.

Table 2. Physical properties of transformer oil [25]

Physical property	Value
Density (kg/m^3)	830
Kinematic viscosity at 100°C (10^{-6} m^2/s)	8.48
Dielectric constant (k_d)	2.1
Dielectric breakdown (kV)	58

The differential equation (17) was solved using MATHEMATICA [26] to obtain the droplet position and velocity with time. Since a published value for the contact-line friction coefficient ζ for transformer oil is not available, a value was chosen that provided the best match to velocity measurements across all the experiments conducted.

3. Experimental characterization of dielectric droplet movement

3.1 Device fabrication

A number of experiments were carried out to benchmark the analytical and numerical models developed in this work. The experiments involved electrical actuation of droplets of

transformer oil (DSI Fluids, Tyler, TX) with a dielectric constant of 2.1. Transformer oil has a very high electrical resistivity of 1.3×10^{14} *ohms-cm* [25] and hence can be considered as a perfectly dielectric liquid. All devices required for experimentation were fabricated in the Birck Nanotechnology Center at Purdue University. Quartz wafers were used as the bottom plates. The actuation electrodes on the bottom plates were made of titanium and were microfabricated using photolithography and wet-etch processes. These electrodes were coated with a Parylene C dielectric layer by a vapor deposition process. The thickness of the Parylene C layer was measured to be 3 *μm* in the devices used for the experiments. The Parylene C -coated devices were then coated with a hydrophobic Teflon layer of approximately 500 *Å* thickness. This was achieved by spinning a 0.1% solution of Teflon-AF 1600 (DuPont, Wilmington, DE) in FC-77 (3M, St. Paul, MN) at 1500 RPM for 30 seconds and a subsequent hard baking process on a hot plate at 95°*C* for 45 minutes. The top plate of the device consisted of an Indium tin oxide-coated glass slide (Delta Technologies, Limited, Stillwater, MN), spin-coated with Teflon. Different desired spacings between the top and bottom plates were achieved with the use of 25 *μm* mica spacers (B & M Co., Inc., Flushing, NY).

3.2 Characterization of droplet motion

The transformer oil droplets were manually dispensed onto one of the actuation electrodes and were then covered with a top plate, with the spacing between the plates determined by the mica spacers. Two different plate spacings of 300 and 500 *μm* were selected for experimentation. The droplet was positioned such that there was a finite overlap with the actuated electrode to initiate the droplet transition. High-speed photography was employed to obtain images of the droplet as it moved to the actuated electrode. The images were processed using MATLAB [27] to yield the droplet position and velocity along the transition. The droplet position was estimated as the average of the leading- and trailing-edge positions at every time instant.

(a)   **(b)**   (c)

Figure 5(a-c) show representative images of a 2 *mm* diameter transformer oil droplet at various stages during its transition between electrodes for a plate spacing of 300 *μm* and an actuation voltage of 1000 *V*.
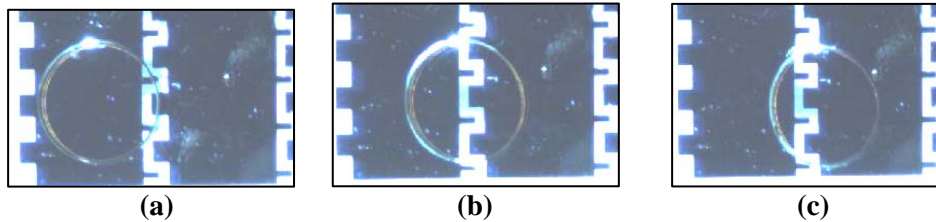

(a)   (b)   (c)

Figure 5. Electrically induced transition of a transformer oil droplet at a) t = 0 s, b) t = 0.8 s, and c) t = 1.73 s(the grounded electrode is on the left and the actuated electrode is on the right).

4. Results and Discussion

4.1 Actuation force on a conducting droplet

The analytical and numerical models developed are first benchmarked by using them to estimate the electrical actuation force on an electrically conducting droplet (with an infinitely large dielectric constant). The predictions are compared with the analytical model of Bahadur and Garimella [2] which was developed for an electrically conducting droplet. It is noted that for

an infinite dielectric constant of the droplet, the expressions resulting from the use of the two analytical approaches developed in this work reduce to the expression for an electrically conducting droplet in [2]. Figure 6 shows the analytical and numerical predictions of the actuation force as a function of the non-dimensional transition distance (normalized using the total transition distance) for an electrically conducting droplet actuated using 50 *V*. A 1 *mm* radius droplet with an infinite dielectric constant sandwiched between two plates with a spacing of 300 *μm* is considered. The numerical results match the analytical model very well, except at the beginning and end of droplet transition; this can be attributed to the electric field fringing effect at the ends. These results serve to benchmark the analytical and numerical models developed in this work for use in predicting the actuation force in dielectric droplets. Figure 6 also shows the results of a mesh-independence study for the numerical model. The actuation force variation was less than 1% when the mesh was refined from $60 \times 60 \times 8$ to $75 \times 75 \times 10$, and therefore, the former mesh was adopted for the predicitons in this work.
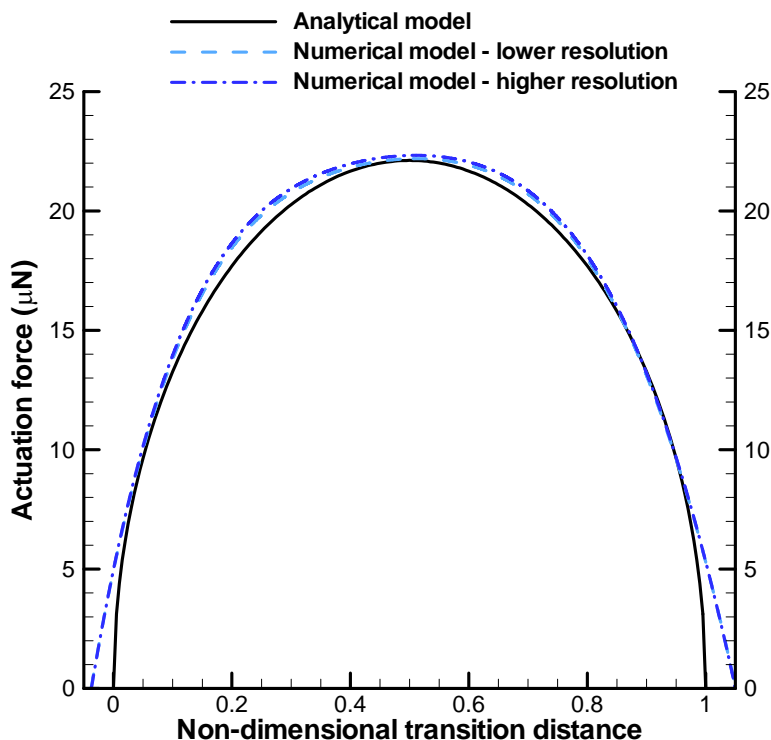

Figure 6. Comparison of analytical and numerical model predictions.

4.2 Actuation force on a dielectric droplet

The actuation force on a dielectric droplet is significantly lower than that on an electrically conducting droplet for a given actuation voltage. Figure 7 shows the actuation force variation with transition distance for a 2 *mm* diameter transformer oil droplet moving between two plates with a spacing of 300 *μm* at an actuation voltage of 1000 *V*. The numerical model shows that the actuation force on the droplet exceeds 20 *μN* for most of the transition distance. Neither of the two analytical approaches replicates the numerical transition force profile; however, the analytical approaches can still provide order-of-magnitude estimates of the actuation force during transition. The analytical results differ significantly from the numerical predictions at the start of the droplet transition. This is because the analysis predicts the actuation force at the start of the droplet transition predominantly based on the energy storage in the capacitive element

10

C_{ae-dl} (the dielectric layer on the actuated electrode on the bottom plate). This is similar to the case of an electrically conducting droplet; thus, the droplet is effectively being modeled as electrically conducting instead of a dielectric at the start of transition. In reality, electric-field fringing results in energy storage in the dielectric droplet even at the beginning of transition. This electric field fringing is captured in the numerical model (but not in the analytical approaches); consequently, the spikes predicted by the analytical approaches at the beginning of transition are not seen in the numerical result. Another point of interest is that the numerical model predicts a small negative force towards the latter stages of the droplet transition which is a consequence of electric field fringing at the end of transition. All the actuation force calculations in the remainder of this paper use the numerical model described here.
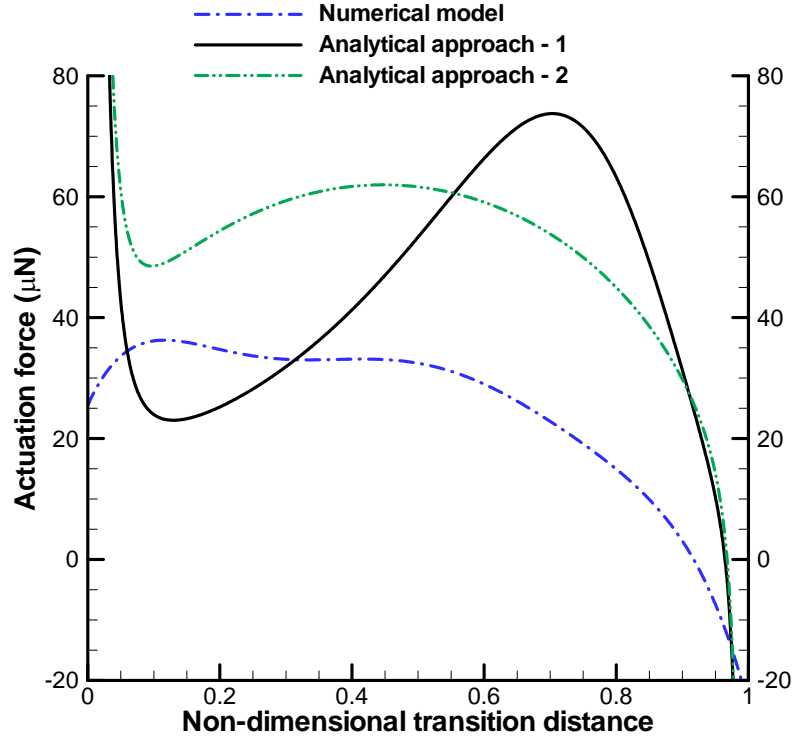

Figure 7. Electrical actuation force prediction using analytical and numerical models for a 1 mm-radius transformer oil droplet (k_d = 2.1) at an actuation voltage of 1000 *V*.

Figure 8 shows the electrical actuation force dependence (using the numerical model) on the droplet dielectric constant for an actuation voltage of 50 *V* and a plate spacing of 300 *μm*. Liquids with three different dielectric constants of 80 (ultra pure water), 25 (ethanol) and 2.1 (transformer oil) are considered. These results are compared with the actuation force on an electrically conducting droplet which corresponds to a dielectric constant value of infinity. It is seen that the actuation force varies strongly with the dielectric constant of the droplet. The magnitude of the actuation force on the dielectric droplets is significantly less than on the electrically conducting droplet. Furthermore, it is seen that the actuation force becomes negative near the end of the transition for all the dielectric constants examined.

A brief discussion of the actuation of water droplets is in order here. Ultra pure water with no ionic impurities would behave as a dielectric droplet with the actuation force predicted as per the k_d = 80 plot in Figure 8. However, in practice, water droplets attract ionic impurities which increases its electrical conductivity significantly. Thus typical water droplets in experiments behave like electrically conducting instead of dielectric droplets, with no voltage

drop across the droplet. This explains the low voltages at which water droplets have been actuated using electrowetting in numerous studies [4, 5].
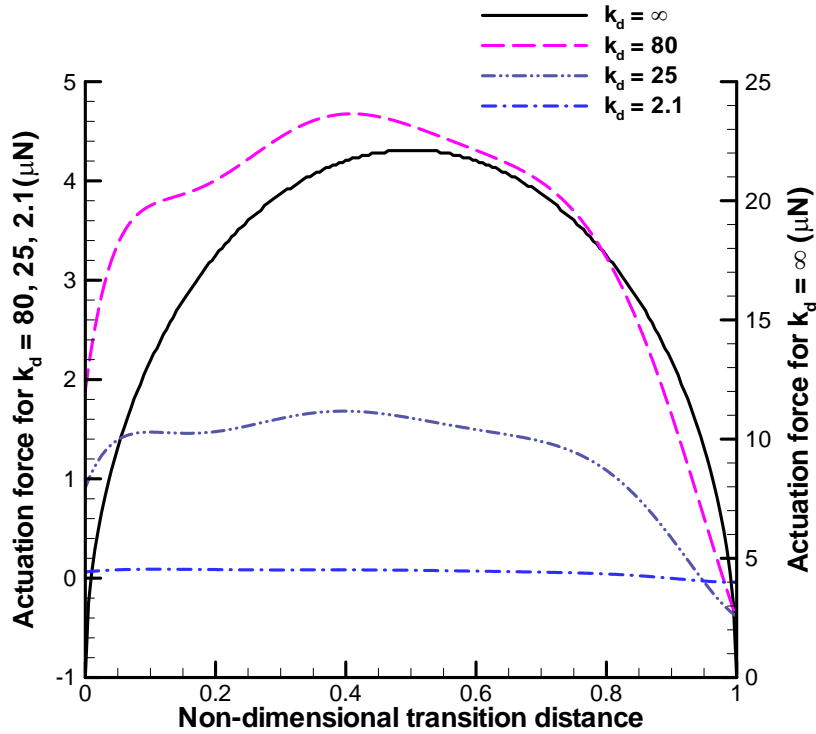

Figure 8. Electrical actuation force dependence on droplet dielectric constant at an actuation voltage of 50 *V*. The y-axis on the right of the plot is used to represent the curve for $k_d = \infty$ for improved resolution.

The effect of plate spacing on the electrical actuation force on a 2 *mm* diameter transformer oil droplet at an actuation voltage of 1000 *V* is illustrated in Figure 9. Three different plate spacing of 100, 300 and 500 *μm* were selected. It is seen that the electrical actuation force decreases as the plate spacing increases which is a direct consequence of a reduction in the electric field with an increase in plate spacing. It is also seen that the position where the transition to a negative force occurs depends on the plate spacing, shifting to the left as the plate spacing is increased. This can be explained directly based on the electric field fringing which increases as the plate spacing is increased.
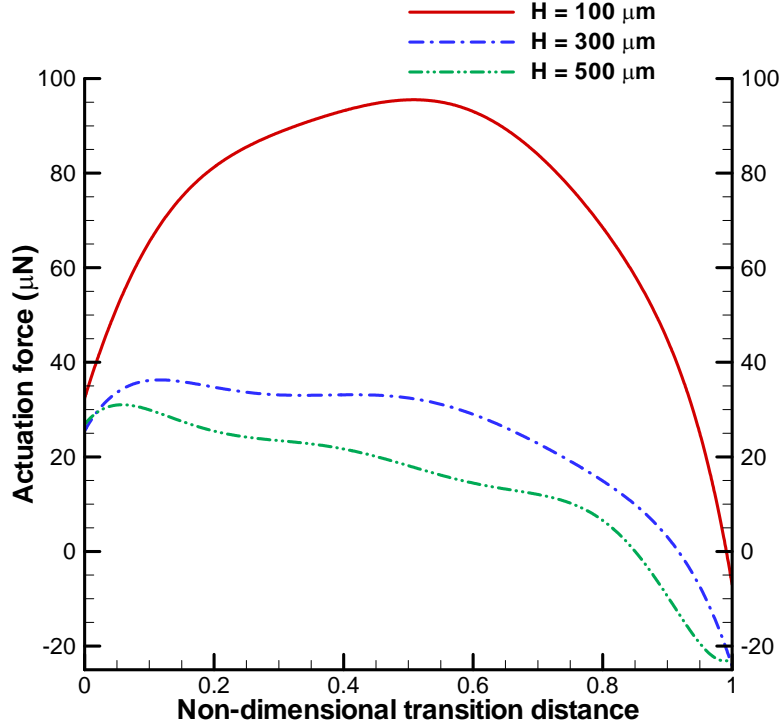
Figure 9. Electrical actuation force dependence on plate spacing for a 1 *mm* transformer oil droplet (k_d = 2.1) at an actuation voltage of 1000 *V*.

4.3 *Validation against experimental droplet motion measurements*

       Representative plots of the experimentally observed velocity variation of a dielectric droplet as it transitions to the actuated electrode for two different plate spacings are shown in Figure 10. The experimental velocities were arrived at by measuring the droplet position as a function of time during the transition.   Table 3 summarizes the experimentally obtained maximum and average velocities resulting from the experiments with different combinations of plate spacings (300 and 500 *μm*) and actuation voltages (1000 and 1500 *V*). In view of the difficulty in making velocity measurements at the start and end of the droplet transition, all velocity measurements in Table 3 consider droplet motion between 30% and 70% of the total transition distance. The typical magnitude of the dielectric droplet velocities is seen to be on the order of 1 *mm/s*, which is 2 orders of magnitude lower than the velocities for electrically conducting droplets [2]. The results shown in Table 3 also indicate that the droplet velocities show a strong dependence on the plate spacing (for identical actuation voltage). A higher plate spacing reduces the electric field which decreases the actuation force as shown in Figure 9; consequently, the droplet velocity is also reduced. The droplet velocity also depends strongly on the actuation voltage which can again be attributed to the dependence of the actuation force on the square of the applied voltage.
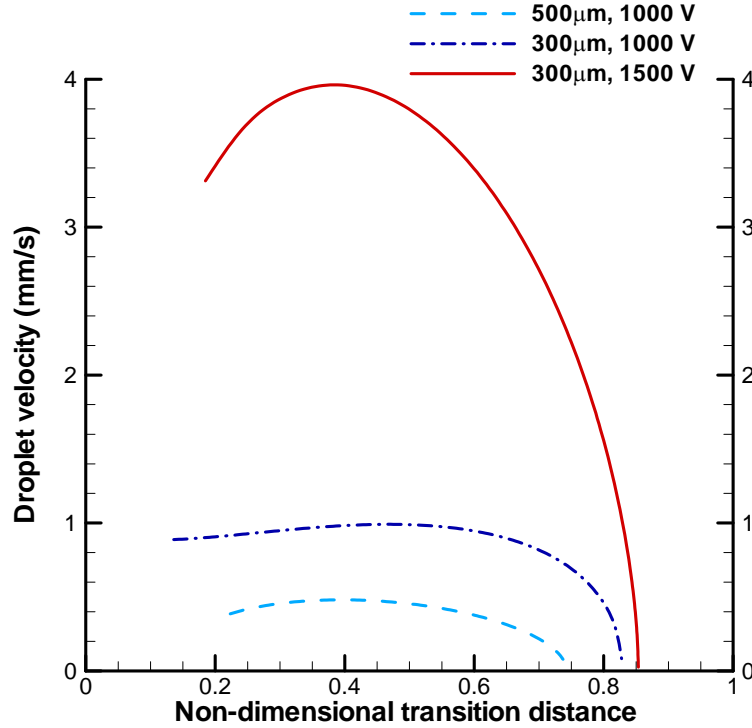
Figure 10. Measured droplet velocities for an electrically actuated transformer oil droplet at different plate spacings and actuation voltages.

Table 3. Experimental measurements of droplet velocity at different plate spacings and actuation voltages (values in parentheses are the numerically predicted velocities).

	d = 500 μm (1000 V)	d = 300 μm (1000 V)	d = 300 μm (1500 V)
Maximum velocity (*mm/s*)	0.41 (0.8)	0.96 (0.86)	3.96 (2.05)
Average velocity between x = 0.3 and 0.7 (*mm/s*)	0.31 (0.47)	0.79 (0.79)	3.52 (1.78)

As mentioned earlier, the contact-line friction coefficient ζ was selected based on a best fit with the experimental results to be 3 *Ns/m²*. It is noted that this value of ζ for transformer oil on Teflon is significantly higher than the value of ζ for water on Teflon (0.04 *Ns/m²*), but is of the same order of magnitude as that of squalene oil (for which $\zeta \approx 1$ *Ns/m²* [28]). Table 3 shows that there are differences between the measured and predicted velocities; however the extent of the agreement between the measured and predicted velocities is considered satisfactory in view of the limitations in the model as well as the experimental uncertainties. The droplet motion model (Eq. (17) with the actuation force estimated using the numerical model) in this work does not account for the existence of a threshold voltage for actuation since this phenomenon is not well understood. The experimental threshold voltage was found to be 700 *V* and this high value indicates the need for its incorporation into droplet motion models. The physics influencing

contact line friction is also not well understood; the first-order estimation of the contact line friction in the present work is partly responsible for the discrepancies between the numerical and experimental velocities. Other contributions to these discrepancies can be attributed to the uncertainties in the plate spacing, droplet radius, droplet volume and initial droplet placement in the experiments.

5. Conclusions

A detailed modeling and experimental study of electrically induced actuation of dielectric droplets is presented. Two analytical approaches are developed and benchmarked against a detailed numerical model to arrive at a first-order estimate of the electrical actuation force on a dielectric droplet as it moves between two flat plates. The numerical actuation force prediction is combined with available semi-analytical expressions for the forces opposing droplet motion to develop a model that predicts transient droplet motion under electrical actuation. The predicted droplet velocities are compared to experimentally measured droplet velocities for a transformer oil droplet moving between two flat plates under an actuation voltage. The influence of plate spacing and actuation voltage on the droplet velocities is experimentally determined. It is seen that dielectric droplets require a much higher actuation voltage to initiate transition as compared to electrically conducting droplets. The measured droplet velocities were also significantly lower than velocities typically encountered during electrowetting-induced actuation of electrically conducting droplets.

References

[1] Mugele F and Baret J C 2005 Electrowetting: from basics to applications *J. of Phys*: *Condensed Matter* **17** R705-R774

[2] Bahadur V and Garimella S V 2006 Energy-based model for electrowetting-induced droplet actuation *Journal of Micromechanics and Microengineering* **16** 1494-1503

[3] Kim C J 2001 Micropumping by electrowetting ASME Int. Mech. Engg. Cong. and Expo. New York IMECE2001/HTD-24200

[4] Pollack M G, Shenderov A D and Fair R B 2002 Electrowetting-based actuation of droplets for integrated microfluidics *Lab on a Chip* 2 96-101

[5] Chatterjee D, Hetayothin B, Wheeler A R, King D J and Garrell R L 2006 Droplet-based microfluidics with nonaqueous solvents and solutions *Lab on a Chip* 6 199-206

[6] Baird E, Young P and Mohseni K 2007 Electrostatic force calculation for an EWOD-actuated droplet *Microfluid Nanofluid* 3 635-644

[7] Oprins H, Vandevelde B, Beyne E, Borghs G and Baelmans M 2004 Selective cooling of microelectronics using electrostatic actuated liquid droplets-modeling and experiments *Intl. Workshop on Thermal Investigations of ICs and Systems Cote d'Azur (France)* 207-212

[8] Pellat H 1895 Mesure de la force agissant sur les diélectriques liquides non électrisés placés dans un champ élitrique *C. R. Acad. Sci Paris* **119** 691-694

[9] Jones T B, Gunji M, Washizu M and Feldman M J 2001 Dielectrophoretic liquid actuation and nanodroplet formation *Journal of Applied Physics* **89** 1441-1448

[10] Pollack M G and Fair R B 2000 Electrowetting-based actuation of liquid droplets for microfluidic applications *Appl. Phys. Lett.* **77** 1725-1726

[11] Mohseni K and Dolatabadi A 2005 Electrowetting droplet actuation in micro scale devices *43rd AIAA Aerospace Sci. Mtg. and Exhibit* Nevada AIAA-677

[12] Kuo J S, Spicar-Mihalic P, Rodriguez I and Chiu D T 2003 Electrowetting-induced droplet movement in an immiscible medium *Langmuir* **19** 250-255

[13] Yi U C and Kim C J 2005 EWOD actuation with electrode-free cover plate *13th Int. Conf. on Solid-State Sensors,Actuators and Microsystems* Seoul (South Korea)

[14] Torkkeli A, Saarilahti J, Haara A, Harma H, Soukka T and Tolonen P 2001 Electrostatic transportation of water droplets on superhydrophobic surfaces *14th Intl. IEEE Conference on MEMS* 475-478

[15] Paik P, Pamula V K and Chakrabarty K 2005 Adaptive hot-spot cooling of integrated circuits using digital microfluidics *Proceedings of IMECE 2005* IMECE2005-81081, Florida(USA)

[16] Bahadur V and Garimella S V 2007 Electrowetting-based control of static droplet states on rough surfaces *Langmuir* **23** 4918-4924

[17] Fair R B, Srinivasan V, Ren H, Paik P, Pamula V K and Pollack M G 2003 Electrowetting-based on-chip sample processing for integrated microfluidics *IEEE Inter. Electron Devices Mtg.*

[18] Quilliet C and Berge B 2001 Electrowetting: a recent outbreak *Current Opinion in Colloid and Interface Sci.* **6** 34-39

[19] Quinn A, Sedev R and Ralston J 2003 Influence of the electrical double layer in electrowetting *J. of Phys. Chem. B* **107** 1163-1169

[20] Blake T D 1993 *Dynamic contact angles and wetting kinetics* in *Wettability, Surfactant Science Series* **49** Marcel Dekker, New York 251-309

[21] Walker S W and Shapiro B 2006 Modeling the fluid dynamics of electrowetting on dielectric (EWOD) *Journal of Microelectromechanical Systems* **15** 986-1000

[22] Carnero C and Carretero J 1996 A study on the physical behaviour of a dielectric slab inserted into a parallel-plate capacitor *Eur. J. Phys.* **17** 220-225

[23] ANSYS 11 Reference Manual 2007, ANSYS Inc.

[24] Ren H, Fair R B, Pollack M G and Shaughnessy E J 2002 Dynamics of electro-wetting droplet transport *Sensors and Actuators B* **87** 201-206

[25] http://www.dsifluids.com/a1.html

[26] MATHEMATICA 5 Reference manual 2005, Wolfram Research Inc., Champaign, IL, USA

[27] MATLAB R2007 Reference manual 2007, The Mathworks, Inc., Natick , MA, USA

[28] Voue M, Rioboo R, Adao M H, Conti J, Bondar A I, Ivanov D A, Blake T D and Coninck J D 2007 Contact-line friction of liquid drops on self-assembled monolayers: chain-length effects *Langmuir* **23** 4695-4699